Journal of Nuclear Materials 380 (2008) 99–104

Contents lists available at ScienceDirect

Journal of Nuclear Materials

journal homepage: www.elsevier.com/locate/jnucmat

Thermodynamic modeling of the U–Mn and U–Nb systems

X.J. Liu, Z.S. Li, J. Wang, C.P. Wang *

Department of Materials Science and Engineering, College of Materials and Research Center of Materials Design and Applications, Xiamen University, Xiamen 361005, PR China

ARTICLE INFO

Article history:
Received 1 March 2008
Accepted 21 July 2008

PACS:
82.60.−s
81.30.Bx

ABSTRACT

The thermodynamic assessments of the U–Mn and U–Nb binary systems were carried out by using the CALPHAD (Calculation of Phase Diagrams) method incorporating experimental thermodynamic properties and phase equilibria. The Gibbs free energies of the liquid, bcc, fcc, αU and βU phases were described by the subregular solution model with the Redlich–Kister equation, and those of the intermetallic compounds (Mn_2U and MnU_6) in the U–Mn binary system were described by the two-sublattice model. The thermodynamic parameters of the U–Mn and U–Nb binary systems were optimized to reproduce the experimental data, and provide agreement with the experimentally determined phase diagram for each binary system.

1. Introduction

The use of uranium in the production of energy from nuclear fission has given considerable impetus to the investigation of the U alloys in recent decades. The investigations of U-based alloys focus not only on the U compounds used in the fuels, but also on the alloys of U and common elements of the structural materials and fission products [1–3]. Mn and Nb are very important alloying elements for the U-based alloys [4–9]. In order to develop new nuclear materials, it is necessary to understand the phase equilibria in U-based alloy systems.

The CALPHAD method is a powerful tool to reduce cost and time during development of materials [10]. As a result, it is of great importance to establish the thermodynamic database for the U-based alloys system. In this paper, as a part of thermodynamic database of U-based alloy systems, the thermodynamic descriptions for the phase equilibria in the U–Mn and U–Nb systems were carried out by means of the CALPHAD method.

2. Thermodynamic model

The information of stable solid phases and the used models in the U–Mn and the U–Nb systems [11] is listed in Table 1.

2.1. Solution phases

The Gibbs free energies of the solution phases in Me–U (Me: Mn, Nb) system were described by the subregular solution model [12]. The molar Gibbs free energy of each solution phase in the Me–U system is given as follows:

$$G^{\phi} = x^0_{\mathrm{Me}} G^{\phi}_{\mathrm{Me}} + x^0_{\mathrm{U}} G^{\phi}_{\mathrm{U}} + RT(x_{\mathrm{Me}} \ln x_{\mathrm{Me}} + x_{\mathrm{U}} \ln x_{\mathrm{U}}) + x_{\mathrm{Me}} x_{\mathrm{U}} \sum_{m=0}^{n} {}^{m}L^{\phi}_{\mathrm{Me,U}} (x_{\mathrm{Me}} - x_{\mathrm{U}})^m, \quad (1)$$

where ${}^0G^{\phi}_{\mathrm{Me}}$ and ${}^0G^{\phi}_{\mathrm{U}}$ are the molar Gibbs free energy of pure element Me and U with the structure ϕ in a nonmagnetic state, which is taken from the compilation by Dinsdale [13] and shown in Table 2. The x_{Me} and x_{U} are the mole fractions of Me and U components, and ${}^mL^{\phi}_{\mathrm{Me,U}}$ is the interaction energy between Me and U atoms, and expressed as:

$${}^{m}L^{\phi}_{\mathrm{Me,U}} = a + bT + cT\ln(T), \quad (2)$$

the parameters of a, b and c are evaluated based on the experimental data in the present work.

2.2. Stoichiometric intermetallic compounds

The Mn_2U and MnU_6 compounds in the U–Mn system are treated as stoichiometric phases. The Gibbs free energy of formation per mole of formula unit $(Mn)_m(U)_n$ can be expressed by the two-sublattice model [14], as the following equation referring to the pure elements in their nonmagnetic state:

$$\Delta G^{\mathrm{Mn}_m\mathrm{U}_n}_f = {}^0G^{\mathrm{Mn}_m\mathrm{U}_n}_f - m\,{}^0G^{\mathrm{ref}}_{\mathrm{Mn}} - n\,{}^0G^{\mathrm{ref}}_{\mathrm{U}} = a' + b'T, \quad (3)$$

where the $\Delta G^{\mathrm{Mn}_m\mathrm{U}_n}_f$ denotes the standard Gibbs free energy of formation of the stoichiometric compound from the pure elements.

* Corresponding author. Tel.: +86 592 2180606; fax: +86 592 2187966.
E-mail address: wangcp@xmu.edu.cn (C.P. Wang).

0022-3115/$ - see front matter © 2008 Elsevier B.V. All rights reserved.
doi:10.1016/j.jnucmat.2008.07.008

Table 1
The stable solid phases and the models used in the U–Mn and U–Nb systems

System	Phase	Prototype	Struckturbericht designation	Modeling phase	Used models
U–Mn	δMn	W	A2	(U,Mn)	Subregular solution model
	γMn	Cu	A1	(U,Mn)	Subregular solution model
	βMn	βMn	A13	(U,Mn)	Subregular solution model
	αMn	αMn	A12	(Mn)	Subregular solution model
	Mn_2U	Cu_2Mg	C15	$(Mn)_2(U)$	Two-sublattice model
	MnU_6	MnU_6	$D2_c$	$(Mn)(U)_6$	Two-sublattice model
	γU	W	A2	(U,Mn)	Subregular solution model
	βU	βU	A_b	(U,Mn)	Subregular solution model
	αU	αU	A20	(U)	Subregular solution model
U–Nb	(γU,Nb)	W	A2	(U,Nb)	Subregular solution model
	βU	βU	A_b	(U,Nb)	Subregular solution model
	αU	αU	A20	(U,Nb)	Subregular solution model

Table 2
Gibbs energy parameters of condensed pure elements [13]

Gibbs free energy (J/mol)	Temperature (K)
Liquid phase	
G_U^{SER}	
$+3947.766 + 120.631251\ T - 26.9182\ T\ln(T) + 1.25156 \times 10^{-3}\ T^2 - 4.42605 \times 10^{-6}\ T^3 + 38\,568\ T^{-1}$	$298.15 < T < 955$
$-10166.3 + 281.797193\ T - 48.66\ T\ln(T)$	$955 < T < 3000$
G_{Mn}^{SER}	
$+9744.63 + 117.4382\ T - 23.4582\ T\ln(T) - 7.34768 \times 10^{-3}\ T^2 + 69\,827\ T^{-1} - 4.41929 \times 10^{-21}\ T^7$	$298.15 < T < 1519$
$-9993.9 + 299.036\ T - 48\ T\ln(T)$	$1519 < T < 2000$
G_{Nb}^{SER}	
$+21262.202 + 131.229057\ T - 26.4711\ T\ln(T) + 2.03475 \times 10^{-4}\ T^2 - 3.5012 \times 10^{-7}\ T^3 + 93\,399\ T^{-1} - 3.06098 \times 10^{-23}\ T^7$	$298.15 < T < 2750$
$-7499.398 + 260.756148\ T - 41.77\ T\ln(T)$	$2750 < T < 6000$
αMn phase	
G_{Mn}^{SER}	
$-8115.28 + 130.059\ T - 23.4582\ T\ln(T) - 7.34768 \times 10^{-3}\ T^2 + 69\,827\ T^{-1}$	$298.15 < T < 1519$
$-28733.41 + 312.2648\ T - 48\ T\ln(T) + 1.656848 \times 1030\ T^{-9}$	$1519 < T < 2000$
βMn phase	
G_{Mn}^{SER}	
$-5800.4 + 135.995\ T - 24.8785\ T\ln(T) - 5.83359 \times 10^{-3}\ T^2 + 70\,269\ T^{-1}$	$298.15 < T < 1519$
$-28290.76 + 311.2933\ T - 48\ T\ln(T) + 3.96757 \times 1030\ T^{-9}$	$1519 < T < 2000$
αU phase	
G_U^{SER}	
$-8407.734 + 130.955151\ T - 26.9182\ T\ln(T) + 1.25156 \times 10^{-3}\ T^2 - 4.42605 \times 10^{-6}\ T^3 + 38\,568\ T^{-1}$	$298.15 < T < 955$
$-22521.8 + 292.121093\ T - 48.66\ T\ln(T)$	$955 < T < 3000$
βU phase	
G_U^{SER}	
$-5156.136 + 106.976316\ T - 22.841\ T\ln(T) - 1.084475 \times 10^{-2}\ T^2 + 2.7889 \times 10^{-8}\ T^3 + 81\,944\ T^{-1}$	$298.15 < T < 941.5$
$-14327.309 + 244.16802\ T - 42.9278\ T\ln(T)$	$941.5 < T < 3000$
Bcc_A2 phase	
G_U^{SER}	
$-752.767 + 131.5381\ T - 27.5152\ T\ln(T) - 8.35595 \times 10^{-3}\ T^2 + 9.67907 \times 10^{-7}\ T^3 + 204\,611\ T^{-1}$	$298.15 < T < 1049$
$-4698.365 + 202.685635\ T - 38.2836\ T\ln(T)$	$1049 < T < 3000$
G_{Mn}^{SER}	
$-3235.3 + 127.85\ T - 23.7\ T\ln(T) - 7.44271 \times 10^{-3}\ T^2 + 60\,000\ T^{-1}$	$298.15 < T < 1519$
$-23188.83 + 307.7043\ T - 48\ T\ln(T) + 1.265153 \times 1030\ T^{-9}$	$1519 < T < 2000$
G_{Nb}^{SER}	
$-8519.353 + 142.045475\ T - 26.4711\ T\ln(T) + 2.03475 \times 10^{-4}\ T^2 - 3.5012 \times 10^{-7}\ T^3 + 93\,399\ T^{-1}$	$298.15 < T < 2750$
$-37669.3 + 271.720843\ T - 41.77\ T\ln(T) + 1.528239 \times 1032\ T^{-9}$	$2750 < T < 6000$
Fcc_A1 phase	
G_U^{SER}	
$-3407.734 + 130.955151\ T - 26.9182\ T\ln(T) + 1.25156 \times 10^{-3}\ T^2 - 4.42605 \times 10^{-6}\ T^3 + 38\,568\ T^{-1}$	$298.15 < T < 955$
$-17521.8 + 292.121093\ T - 48.66\ T\ln(T)$	$955 < T < 3000$
G_{Mn}^{SER}	
$-3439.3 + 131.884\ T - 24.5177\ T\ln(T) - 0.006\ T^2 + 69\,600\ T^{-1}$	$298.15 < T < 1519$
$-26070.1 + 309.6664\ T - 48\ T\ln(T) + 3.86196 \times 1030\ T^{-9}$	$1519 < T < 2000$

The terms ${}^0G_{Mn}^{ref}$ and ${}^0G_U^{ref}$ are the molar Gibbs free energy of pure element Mn and U with its defined reference structure in a nonmagnetic state. The parameters of a' and b' are evaluated in the present optimization.

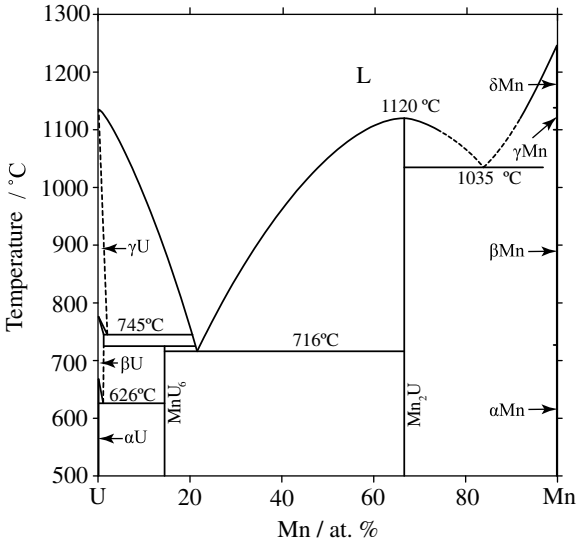

Fig. 1. The phase diagram of the U–Mn system reviewed by Massalski et al. [17].

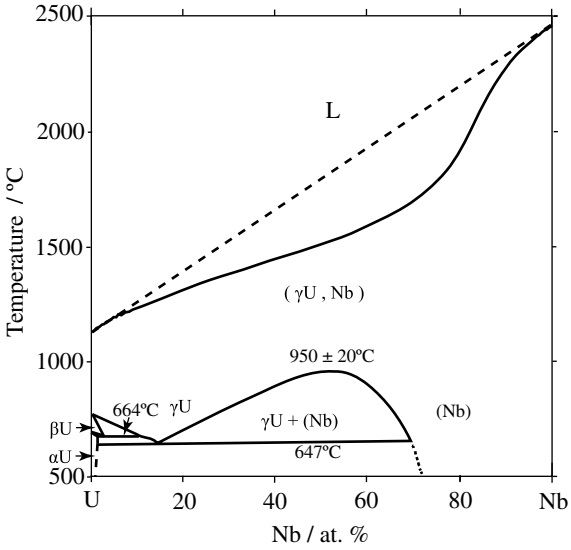

Fig. 2. The phase diagram of the U–Nb system reviewed by Koike et al. [31].

3. Experimental information

3.1. The U–Mn system

The phase diagram of the U–Mn system consists of seven solution phases (αMn, βMn, γMn, δMn, αU, βU, γU), and two intermetallic compounds (MnU_6 and Mn_2U phases). The phase diagram in the U–Mn system was originally proposed by Wilhelm and Carlson [15], and then reassessed by Hanse et al. [16] and Massalski [17]. The maximum solubility of Mn in the γU phase was estimated to be less than 1 wt% based on metallography. Although the solubilities of U in all the allotropes of Mn have not been investigated thoroughly, some solid solubilities were found by Whilhelm using X-ray studies [15]. The Mn_2U phase has three polymorphs: αMn_2U, βMn_2U and γMn_2U. The polymorphic transformation temperatures of the $\gamma Mn_2U \leftrightarrow \beta Mn_2U$ and $\beta Mn_2U \leftrightarrow \alpha Mn_2U$ were respectively reported to be −61 °C and −161 °C [17]. Because these transformation temperatures of the Mn_2U phase were too low to use in the present assessment, the Mn_2U phase is treated as one stoichiometric phase. The phase diagram of the U–Mn system reviewed by Massalski [17] is shown in Fig. 1.

In addition, the enthalpies and entropies of formation of the compounds (MnU_6 and Mn_2U) in the temperature range from 660 °C to 860 °C were determined by Lebedev et al. [18] on the basis of Electromagnetic Fields (EMF) measurements.

3.2. The U–Nb system

The U–Nb system consists of three solution phases (αU, βU and (γU, Nb)), and a phase separation (γU + (Nb)) in the bcc phase at lower temperature. The phase diagram in the U–Nb system has been investigated by many researchers [16,19–31]. There are two different conclusions for the monotectoid reaction of γU in this system as follows: the reaction of $\gamma U \leftrightarrow (Nb) + \alpha U$ was reported

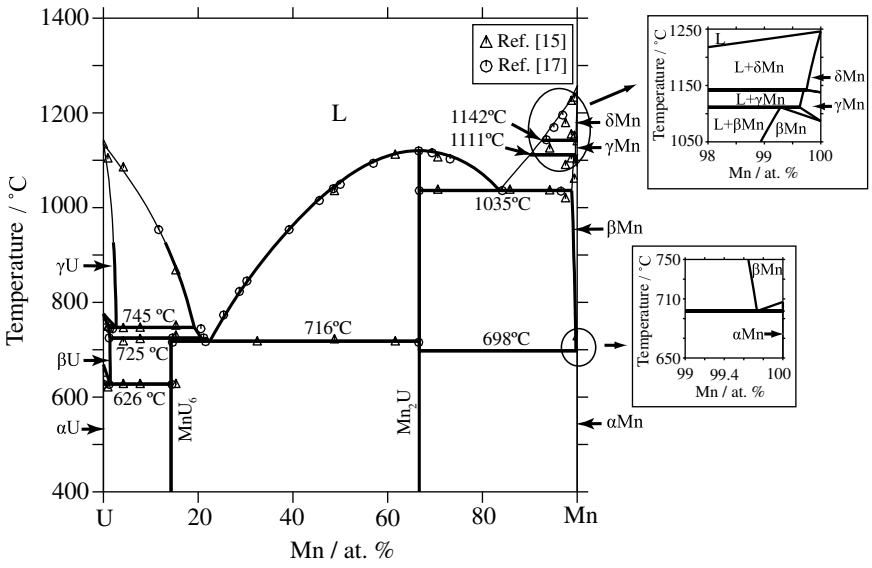

Fig. 3. Calculated phase diagram of U–Mn binary system with experimental data [15,17].

by Roger et al. [16,22,25,28], and the γU ↔ (Nb) + βU was reported by Terekhov [29]. Massalski [17] reviewed the phase diagram according to Rogers [22] and Terekhov [29], where the monotectoid reaction of the γU ↔ (Nb) + βU is accepted [29]. However, in the Koike review [31], the monotectoid reaction of the γU ↔ Nb + αU is adopted according to the previous work [16,17,19–28,30]. The liquidus line was only estimated by Rogers [22], because of the difficulty in the experiment. In this work, the assessment was carried out on the basis of the experiment data by [17,21–23,30], and the monotectoid reaction of the γU ↔ (Nb) + αU was adopted. The phase diagram reviewed by Koike, et al. [31] is shown in Fig. 2.

In addition, the physical properties such as the Debye temperature and Young's modulus of the solid solution alloys were determined based on the fused salt EMF measurements by Fedorov and Smirnov [32] and by Vamberskij et al. [33]. Vamberskij et al. [33] also calculated Gibbs free energies of formation of the U–Nb system at 775 °C and 900 °C by the Gibbs–Duhem equations according to their experimental data.

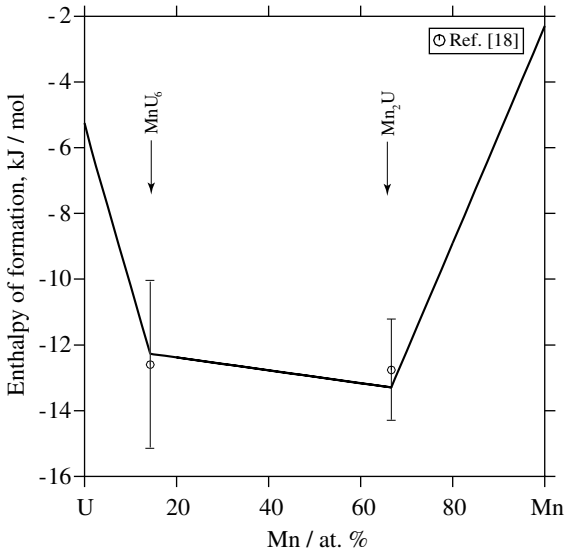

Fig. 4. Calculated enthalpies of formation of intermetallic compounds at 677 °C in the U–Mn system compared with the experimental data [18]: the reference states are γU phase and βMn phase.

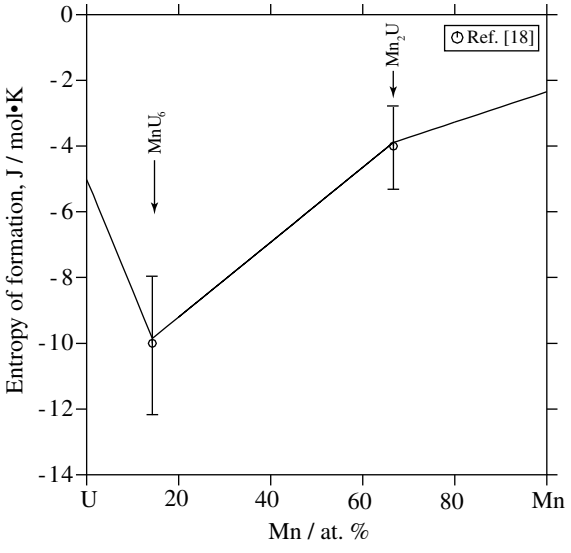

Fig. 5. Calculated entropies of formation intermetallic compounds at 677 °C in the U–Mn system compared with the experimental data [18]: the reference states are γU phase and βMn phase.

4. Optimized results and discussion

Optimization of thermodynamic parameters describing the Gibbs free energies of each phase is carried out using PARROT [34] module in the Thermo-Calc software [35], a computer program that can accept different types of data, such as any specific thermodynamic quantities and phase equilibria, in the same operation. Each piece of the selected data is given a certain weight and

Table 3
Thermodynamic parameters for the U–Mn system optimized in this work

Parameters in each phase (J/mol)
Liquid phase, format (Mn,U)$_1$
${}^0L^{Liq}_{Mn,U} = -23400 + 11.7T$
${}^1L^{Liq}_{Mn,U} = 320 - 1.77T$
${}^2L^{Liq}_{Mn,U} = -10966 + 10.4T$
A2 (γU,δMn) phase, format (Mn,U)$_1$(Va)$_3$
${}^0L^{bcc}_{Mn,U} = 11000 + 9.83T$
${}^1L^{bcc}_{Mn,U} = 2800 + 4.7T$
A$_b$ βU phase, format (Mn,U)$_1$
$G^{\beta U}_{Mn} = G^{\gamma Mn}_{Mn} + 25000$
${}^0L^{\beta U}_{Mn,U} = 29614.8 - 12.5T$
${}^1L^{\beta U}_{Mn,U} = 69425 - 48.7T$
${}^2L^{\beta U}_{Mn,U} = -49519.7 + 47.07T$
A1 γMn phase, format (Mn,U)$_1$(Va)$_1$
${}^0L^{fcc}_{Mn,U} = 25000$
A13 βMn phase, format (Mn,U)$_1$(Va)$_1$
$G^{\beta(Mn)}_{U} = G^{\gamma U}_{U} + 5000$
${}^0L^{\beta Mn}_{Mn,U} = 7971 + 6.97T$
Mn_2U phase, format (Mn)$_{0.6667}$ (U)$_{0.3333}$
$G^{Mn_2U}_{Mn:U} = 0.6667G^{\gamma Mn}_{Mn} + 0.3333G^{\gamma U}_{U} - 9100 - 0.32T$
MnU_6 phase, format (Mn)$_{0.1429}$ (U)$_{0.8571}$
$G^{MnU_6}_{Mn:U} = 0.1429G^{\gamma Mn}_{Mn} + 0.8571G^{\gamma U}_{U} - 5090 + 2.71T$

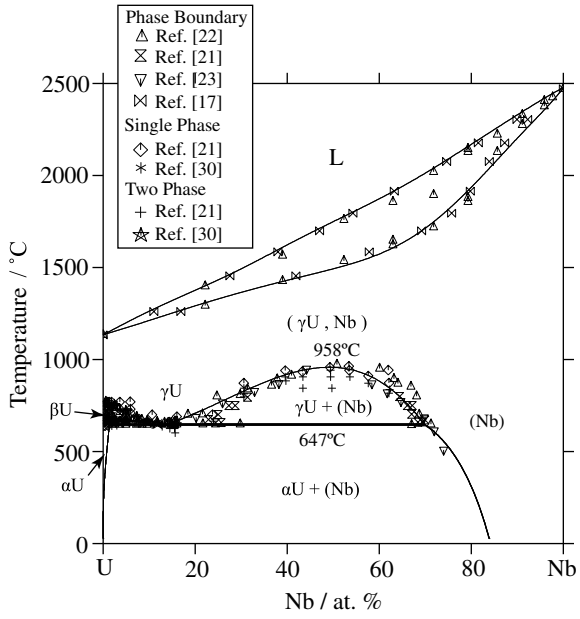

Fig. 6. Calculated phase diagram of U–Nb binary system with experimental data [17,21–23,30].

Table 4
A comparison of calculated invariant reactions and special points in the U–Mn system with experimental results

Reaction type	Reaction	Mn (at.%)			T (°C)	References
Catatectic	γU → βU + L	2.3	1.2	20.6	745	[17]
		2.7	1.22	19.3	745	[This work]
Peritectic	βU + L → MnU_6	1.2	21.5	14.3	725	[17]
		1.3	21	14.3	725	[This work]
Eutectoid	βU → αU + MnU_6	1.2	0	14.3	626	[17]
Eutectic	L → MnU_6 + Mn_2U	21.5	14.3	66.7	716	[17]
		22.6	14.3	66.7	716	[This work]
Eutectic	L → βMn + Mn_2U	84	–	66.7	1035	[17]
		83.7	98.9	66.7	1035	[This work]
Melting	L → Mn_2U		66.7		1120	[17]
			66.7		1120	[This work]
Peritectic	δMn + L → γMn	–	–	–	–	–
		99.7	92.5	99.8	1142	[This work]
Peritectic	γMn + L → βMn	–	–	–	–	–
		99.6	90.1	99.3	1111	[This work]
Eutectoid	βMn → αMn + Mn_2U	–	–	–	–	–
		99.7	1	66.7	698	[This work]

the weight can be changed until a satisfactory description for most of the selected data is achieved.

4.1. The U–Mn system

The calculated phase diagram of the U–Mn system compared to all the experimental data [15,17] used in the present optimization is shown in Fig. 3. It is seen from Fig. 3 that the calculated results are in agreement with Massalski [17], but there are some differences with Wilhelm [15] in the Mn-rich region. The calculated largest solid solubilities of U in the βMn, γMn and δMn phases are respectively 0.7 at.%, 0.4 at.% and 0.3 at.%. In the Mn-rich region, a little solubility of U in the βMn and γMn was given in this work, although there are no experimental data about this point. The calculated enthalpies and entropies of formation of the compounds with the experimental data at 677 °C are shown in Figs. 4 and 5. The calculated results are in good agreement with the experimental data [18].

A complete set of the thermodynamic parameters describing the Gibbs free energy of each phase, including the elements as well, is given in Table 3. And all invariant reactions and special points in the U–Mn system are summarized in Table 4, in which the experimental data are also listed for comparison [17]. The calculated congruent melting temperature of the Mn_2U phase and the eutectic temperatures are in agreement with the corresponding experimental data [18].

4.2. The U–Nb system

The calculated U–Nb phase diagram with the experimental data is shown in Figs. 6 and 7. The calculated phase diagram, especially the phase boundary of miscibility gap region (γU + Nb), is in agreement with the experimental data [17,21–23,30]. The calculated liquidus line agrees with Rogers [22] and the Massalski review [17]. Figs. 8 and 9, respectively indicate the calculated Gibbs free energies at 775 °C and 900 °C compared with the data obtained from the Gibbs–Duhem equations [33]. It is seen from Figs. 8 and 9 that there are some differences between the present calculated results and data reported by Vamberskij [33]. In particular, in the

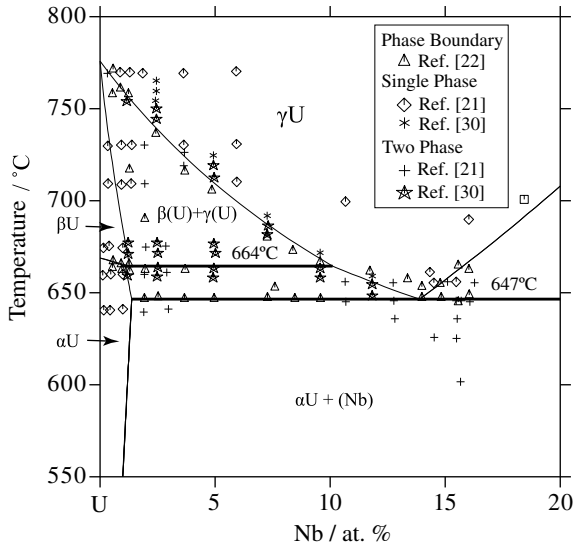

Fig. 7. Calculated phase diagram of U–Nb binary system in the U-rich portion with experimental data [21,22,30].

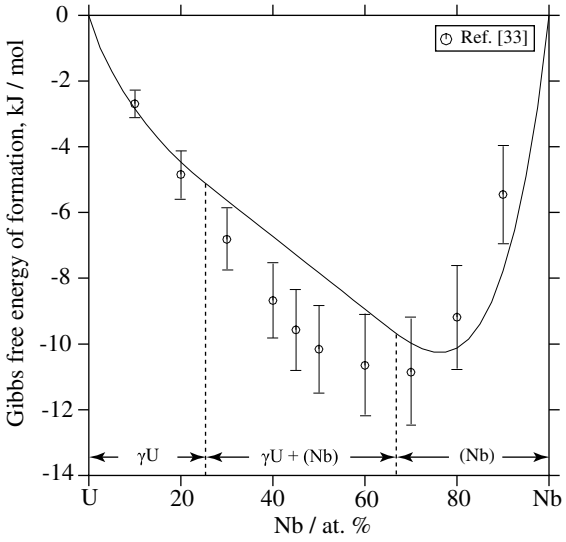

Fig. 8. Calculated Gibbs free energy at 775 °C in the U–Nb system compared with the calculation data by Vamberskij et al. [33]: the reference states are bcc γU phase and bcc (Nb) phase.

Table 5
Thermodynamic parameters for the U–Nb system optimized in this work

Parameters in each phase (J/mol)
Liquid phase, format (Nb,U)$_1$
${}^0L^{Liq}_{Nb,U} = 39836.8 - 41.2T$
${}^1L^{Liq}_{Nb,U} = -149230.3 + 47.2T + 4.66T\ln(T)$
${}^2L^{Liq}_{Nb,U} = -38091.3 - 4.33T$
A2 (γU,Nb) phase, format (Nb,U)$_1$(Va)$_3$
${}^0L^{bcc}_{Nb,U} = 17706.2 - 23.099T$
${}^1L^{bcc}_{Nb,U} = -54699.5 + 30.02T$
${}^2L^{bcc}_{Nb,U} = -42938.27 + 9.6T$
${}^3L^{bcc}_{Nb,U} = -28942 + 11.06T$
A_b βU phase, format (Nb,U)$_1$
$G^{\beta U}_{Nb} = G^{bcc}_{Nb} + 15000$
${}^0L^{\beta U}_{Nb,U} = 4018.4$
A20 αU phase, format (Nb,U)$_1$
$G^{\alpha U}_{Nb} = G^{bcc}_{Nb} + 25000$
${}^0L^{\alpha U}_{Nb,U} = -5000$

Table 6
A comparison of calculated invariant reactions and special points in the U–Nb system with experimental results

Reaction type	Reaction	Nb (at.%)			T (°C)	References
Eutectoid	βU → αU + γU	1.3	0.5–0.9	10.5∼11.5	664	[31]
		1.3	1.09	10.1	664	[This work]
Monotectoid	γU → αU + (Nb)	13.3	0.5	68∼72	647	[31]
		13.9	1.3	70	647	[This work]
Critical	(γU, Nb) → γU + (Nb)		52.3		930–970	[31]
			50.7		958	[This work]

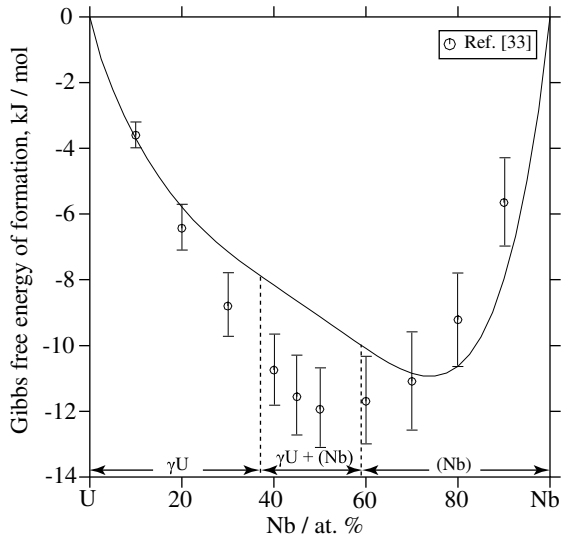

Fig. 9. Calculated Gibbs free energy at 900 °C in the U–Nb system compared with the calculation data by Vamberskij et al. [33]: the reference states are bcc γU phase and bcc (Nb) phase.

γU + (Nb) miscibility gap region, the calculated Gibbs free energies are higher than ones by Vamberskij. However, the present calculations are reasonable by considering the error range of Vamberskij's data.

A complete set of the thermodynamic parameters describing the Gibbs free energy of each phase in this system is given in Table 5, and all invariant reactions in the U–Nb system are summarized in Table 6, in which the experimental data are also listed for comparison [31].

5. Conclusions

The phase diagrams and thermodynamic properties in the U–Mn and U–Nb binary systems were evaluated by combining the thermodynamic models with the available experimental information in literature. A consistent set of optimized thermodynamic parameters has been derived for describing the Gibbs free energy of each solution phase and intermetallic compounds in the U–Mn and U–Nb binary systems. Good agreement between the calculated results and most of the experimental data is obtained.

Acknowledgements

This work was supported by the National Natural Science Foundation of China (Nos. 50425101 and 50771087) and Fujian Provincial Department of Science and Technology (Grant No. 2002I018), and Xiamen Bureau of Science and Technology (Grant No. 02Z20055016). One of the authors (X.J. Liu) acknowledges the Minjiang Chair Professorship by Fujian Province of PR China for financial support.

References

[1] C. Guéneau, S. Chatain, S. Gossé, C. Rado, O. Rapaud, J. Lechelle, J.C. Dumas, C. Chatillon, J. Nucl. Mater. 344 (2005) 191.
[2] R. Schmid-Fetzer, D. Andersson, P.Y. Chevalier, L. Eleno, O. Fabrichnaya, U.R. Kattner, B. Sundman, C. Wang, A. Watson, L. Zabdyr, M. Zinkevich, Comput. Coupling Phase Diagr. Thermochem. 31 (2007) 38.
[3] C. Degueldre, C. Guéneau, J. Nucl. Mater. 352 (2006) ix.
[4] R. Jerlerud Pérez, A.R. Massih, J. Nucl. Mater. 360 (2007) 242.
[5] C. Ramos, C. Saragovi, M.S. Granovsky, J. Nucl. Mater. 366 (2007) 198.
[6] GM. Ludtka, Metall. Trans. 24A (1993) 379.
[7] V.K. Shamardin, T.M. Bulanova, V.N. Golovanov, V.S. Neustroyev, A.V. Povstyanko, Z.E. Ostrovsky, J. Nucl. Mater. 233–237 (1996) 162.
[8] Y. Suzuki, T. Saida, F. Kudough, J. Nucl. Mater. 258–263 (1998) 1687.
[9] E.T. Cheng, G. Saji, J. Nucl. Mater. 212–215 (1994) 621.
[10] L. Kaufman, H. Bernstein, Computer Calculation of Phase Diagram, Academic Press, New York, 1970.
[11] H. Okamoto, Desk Handbook-Phase Diagrams for Binary Alloys, ASM International, 2000.
[12] H.K. Hardy, Acta Metall. (1) (1953) 202;
H.K. Hardy, Acta Metall. (2) (1954) 348.
[13] A.T. Dinsdale, CALPHAD 15 (1991) 317.
[14] M. Hillert, L.I. Stafansson, Acta. Chem. Scand. 24 (1970) 3618.
[15] H.A. Wilhelm, O.N. Carlson, Trans. ASM 42 (1950) 1311.
[16] M. Hansen, K. Anderko, Constitution of Binary Alloys, McGraw-Hill, New York or General Electric Co., Business Growth Services, Schenectady, New York, 1958.
[17] T.B. Massalski, P.R. Subramanian, H. Okamoto, L. Kacprzak, ASM Int. 1990.
[18] V.A. Lebedev, V.I. Lyazgin, A.V. Ishutin, I.F. Nichkov, S.P. Raspopin, Russ. Metall. 2 (1973) 160.
[19] H.A. Saller, E.A. Rough, US Atom. Energy Comm. BMI-1000 (1955) 48.
[20] A.E. Dwight, M.H. Mueller, US Atom. Energy Comm. ANL-5581(1957).
[21] P.C.L. Pfeil, J.D. Browne, G.K. Williamson, J. Inst. Metals. 87 (1958) 204.
[22] B.A. Rogers, D.F. Atkins, E.J. Manthos, M.E. Kirkpatrick, Trans. Metall. Soc. AIME 212 (1958) 387.
[23] O.S. Ivanov, G.I. Terekhov, US Atom. Energy Comm. 18–32 (1961).
[24] A.D. Roming, Sandia Rep. SAND-86-0906C, Albuquerque, NM (1986).
[25] R.P. Elliott, Constitution of Binary Alloys, First Supplement, McGraw-Hill, New York, 1965.
[26] F.A. Shunk, Constitution of Binary Alloys, Second Supplement, McGraw-Hill, New York, 1969.
[27] P. Feschotte, D.T. Livey, O. von Goldbeck, Atomic Energy Review, Special Issue No. 2, IAEA, Vienna (1968), 45.
[28] P. Chiotti, V.V. Akhachinskij, I. Ansara, The Chemical Thermodynamics of Actinide Elements and Compounds, Part 5: The Actinide Binary Alloys, in: V. Medvedev, M.H. Rand, E.F. Westrum Jr., F.L. Oetting (Eds.), International Atomic Energy Agency, Vienna, 1981.
[29] G.I. Terekhov, Russ. Metall. 4 (1982) 170.
[30] C. Fizzotti, A. Maspereni, Com. Naz. Energ. Nucl. RTIMET(66)-1 (1966) 1.
[31] J. Koike, M.E. Kassner, R.E. Tate, R.S. Rosen, Phase Diagrams of Binary Actinide Alloys, in: M.E. Kassner, D.E. Peterson (Eds.), ASM International, Materials Park, OH, 1995.
[32] G.B. Fedorov, E.A. Smirnov, Sov. J. Atom. Energy. 21 (1966) 837.
[33] Y.V. Vamberskij, A.L. Udovskij, O.S. Ivanov, J. Nucl. Mater. 55 (1975) 96.
[34] B. Jansson, Ph.D. Thesis, Division of Physical Metallurgy, Royal Institute of Technology, Stockholm, Sweden, 1984.
[35] B. Sundman, B. Jansson, J.O. Andersson, CALPHAD 9 (1985) 153.